2022-01-0921 Published 29 Mar 2022

Electric Vehicle Corner Architecture: Driving Comfort Evaluation Using Objective Metrics

Vidas Žuraulis and Paulius Kojis Vilnius Gediminas Technical University

Raffaele Marotta Università Degli Studi di Napoli

Šarūnas Šukevičius and Eldar Šabanovič Vilnius Gediminas Technical University

Valentin Ivanov Technische Universitat Ilmenau

Viktor Skrickij Vilnius Gediminas Technical University

Citation: Žuraulis, V., Kojis, P., Marotta, R., Šukevičius, Š. et al., "Electric Vehicle Corner Architecture: Driving Comfort Evaluation Using Objective Metrics," SAE Technical Paper 2022-01-0921, 2022, doi:10.4271/2022-01-0921.

Received: 24 Jan 2022 Revised: 24 Jan 2022 Accepted: 10 Jan 2022

Abstract

The presented paper is dedicated to the driving comfort evaluation in the case of the electric vehicle architecture with four independent wheel corners equipped with in-wheel motors (IWMs). The analysis of recent design trends for electrified road vehicles indicates that a higher degree of integration between powertrain and chassis and the shift towards a corner-based architecture promises improved energy efficiency and safety performances. However, an in-wheel-mounted electric motor noticeable increases unsprung vehicle mass, leading to some undesirable impact on chassis loads and driving comfort. As a countermeasure, a possible solution lies in integrated active corner systems, which are not limited by traditional active suspension, steer-by-wire and brake-by-wire actuators. However, it can also include actuators influencing the wheel positioning through the active camber and toe angle control. Such a corner configuration is discussed in the paper as applied to a sport utility vehicle (SUV). A new chassis design was developed and tested for this reference vehicle using multi-body dynamics simulation. The integrated operation of the active suspension and the wheel positioning control has been analyzed in this study with different driving scenarios and objective metrics for driving comfort evaluation. Additionally, handling and stability tests have also been performed to confirm that new systems do not deteriorate driving safety. The obtained results contribute to a comprehensive assessment of IWM-based architecture, formulated from a driving comfort perspective that is helpful for further designs of electric vehicle corners.

1. Introduction

Many recent technological trends in road vehicle electrification are closely connected to a growing interest in IWMs from the side of automotive original equipment manufacturers (OEMs) and suppliers [1]. IWMs can bring many benefits related to more agile motion control, driving safety, and the flexibility of powertrain topology in general. Of particular importance for the automotive chassis design is the fact that an IWM can be considered as a multipurpose actuator, which is simultaneously applicable for the control on longitudinal, lateral and vertical dynamics that was clearly demonstrated in [2, 3]. These features of IWMs also motivated engineers to investigate new designs of the vehicle architecture represented by active wheel corner concepts, where chassis systems as brake-by-wire, steer-by-wire and active dampers are being integrated in the wheel hub space. Despite the first active wheel corner concepts that arose over a decade ago [4, 5], they are becoming more important with emerging down-sized chassis actuators.

Several studies reported that the electric vehicle topology with IWMs is beneficial for vehicle stability and energy efficiency [6-8]. However, the use of IWMs can negatively influence the ride quality due to the increased unsprung mass of the vehicle. For instance, this aspect was thoroughly discussed in [9, 10]. Moreover, the use of wheel motors on an electric vehicle causes lower natural vertical frequency but higher acceleration magnitude of unsprung mass [11]. This factor leads to potential deterioration of vehicle comfort as the human body is sensitive to the 4-8 Hz frequency range [12]. A (semi-)active suspension can compensate for the adverse effects of higher unsprung mass for both ride comfort and road holding capability but mainly at low driving velocities; however, the losses in road holding usually occur at higher velocities. Some works propose the optimization of the

suspension stiffness and damping values according to the vehicle weighted vertical acceleration and the pitching angle acceleration to improve only ride comfort of an electric vehicle with IWMs [13]. This study has determined significantly lower suspension stiffness and damping values after multi-objective optimization, leading to the best reduction of weighted acceleration for 70 km/h (–12.71%) and the lowest for 100 km/h (–4.75%). Another research dealing with the same issue of IWMs proposes a so-called discomfort criterion based on suspension travel [14]. The results show that rear suspension and driver's seat stiffness mainly influence ride comfort. However, whole vehicle suspension damping has the main impact on the wheel travel and suspension construction design.

A design of dynamic vibration absorber for IWM by [15] was used to compare the performance of an alternative two-stage suspension design for the same in-wheel structure of electric vehicles [16]. The lower value of unsprung mass vertical acceleration was obtained using a specific in-wheel added suspension, although the body and vertical wheel accelerations were not reduced. An active motor vibration-absorbing system with multi-stage passive vibration-isolating inside the wheel rim was also suggested instead of modifying existing suspension construction to improve the ride comfort and safety [17]. Additional 40 kg of mass in the case of in-wheel electric vehicle architecture with switch reluctance motor instead of permanent magnet motor was analyzed using quarter-car suspension model of McPherson strut type in [18]. In this example, the vehicle body for each quarter was 20 kg heavier than conventional vehicles because of the battery weight. Both velocity amplitude and displacement of sprung and unsprung masses were found higher for 16-25% for an electric vehicle IWMs; however, according to frequency analysis, the system performance did not cross below 1-1.5 Hz theoretically means safe enough design. Another specific issue of switch reluctance motors' application at in-wheel corner architecture is highlighted as high torque ripple, which produces significant vertical force fluctuations [19]. The main issue is that the frequency of the motor's generated vertical force covers natural frequencies of vehicle sprung and unsprung mass (when it is an in-wheel architecture), causing deterioration in the ride comfort and tire-road contact.

2. Proposed Vehicle Architecture

2.1. Target Vehicle

The vehicle type of Sport Utility Vehicle was built in the MSC Adams/Car multi-body dynamics simulation platform using vehicle 3D model. The model was parameterized using technical data of the reference vehicle provided by the OEM. McPherson strut for front and multi-link with trailing arm and subframe for rear suspension was built with CAD shaped parts added on an appropriate template. Both axles are equipped with anti-roll bars. Inertia parameters for parts were calculated according to the shape and material selected (steel and aluminium). Rack-pinion steering type according to manufactured design was used for steering subsystem. Force elements corresponding to suspension springs and dampers were described by non-linear characteristics measured and created as a property file in advance. The vehicle body was added only by the appropriate center of gravity (CoG), inertia and aerodynamics parameters, and the brakes were adapted using necessary parameters from MSC Adams/Car library as a less relevant subsystem for current research. The body mass corresponding to the vehicle sprung mass is kept as 1869 kg, resulting in the ratio of unsprung/sprung mass of 0.095 and 0.17 for the conventional and IWM-based vehicle architectures, respectively.

As the main object of this research, a modified rear vehicle suspension with IWMs was developed (Fig. 1). The mounting of the original chassis parts was implemented by appropriate hardpoint locations, joints and bushings in the multi-body model; however, a necessary correction for hardpoints corresponding to the front and rear lower control arm and hub mounting for both rear axle corners was done because of the new hub design with an IWM added. The hardpoints of new components to the body remain unchanged. As a result, new design solutions can be realized on a real car without significant chassis modifications. The main kinematical and inertial parameters of the reference vehicle and designed corner are provided in Table 1. Only unsprung mass changes significantly; however, it influences the performance of vertical vehicle dynamics as natural frequencies to change according to relations:

FIGURE 1 CAD model of vehicle rear suspension with IWMs.

TABLE 1 Main suspension characteristics.

Parameter	Reference Vehicle	New Corner Design
Rear wheel track (mm)	1631	1631
Rear wheel displacement (mm)	249	247,5
Caster (degrees)	from 4.6 to 5.8	from 4.5 to 5.75
Camber (degrees)	from -0.75 to 1.38	from -0.85 to 1.5
Toe (degrees)	from -0.53 to -0.25	from -0.51 to 0.35
Unsprung mass (kg)	44.40	79.20

$$\omega_{o,s} = \sqrt{\frac{k_{sp}k_{tr} / \left(k_{sp} + k_{tr}\right)}{m_s}}, \quad (1)$$

$$\omega_{o,us} = \sqrt{\frac{k_{sp} + k_{tr}}{m_{us}}}, \quad (2)$$

where: k_{sp} is the suspension stiffness, k_{tr} is the tire stiffness, m_s is the sprung mass, m_{us} is the unsprung mass. These are undamped natural frequencies ($\omega_{o,i}$), and quarter car sprung mass is used; however, the damped natural frequencies will be slightly lower due to system damping properties. As a part of unsprung mass, the IWM reduces the natural frequency of unsprung mass (2) and does not directly influence the natural frequency of sprung mass (1).

2.2. Objective Metrics and Difference Thresholds

In this study, the driving comfort is being analyzed from the vehicle's vibrations perspective. A vehicle occupant feels vibrations transmitted only from the sprung mass; therefore, discomfort can be minimized by properly designing vehicle systems, the most important of which is suspension. However, unsprung mass oscillation indirectly impacts the driving comfort that should be considered during the design process. Objective metrics for comfort evaluation are available in the literature [12, 20-26]. In this study, international standard ISO 2631-1 [12] for weighting vertical acceleration signals was utilized according to the vertical direction of excitation. Gräbe et al. [27], in their experimental investigation, found that the vertical component ride value is sufficient to quantify discomfort arising from vehicle vibrations. The vibration evaluation is defined by the frequency weighted root-mean-square (RMS) acceleration:

$$a_{z,w} = \sqrt{\frac{1}{T}\int_0^T a_{z,w}^2(t)\,dt}, \quad (3)$$

where: T is the duration of measurement; $a_{z,w}(t)$ is the weighted acceleration as a function of time for the vertical direction.

The RMS values for unweighted and weighted acceleration are slightly different because of frequency weighting *Wk* applied according to human body sensitive frequencies (Fig. 2). The deterioration of ride comfort level with increasing excitation frequency (driving speed) is not uniform because of suspension characteristics and sprung - unsprung mass ratio.

International standard [12] does not provide vibration exposure limits, but it helps to determine the levels of vibrations to which exposure will be acceptable to humans. The scope of this standard considers specific frequency ranges: 0.1 Hz to 0.5 Hz for motion sickness and 0.5 Hz to 80 Hz for health, comfort and perception. An objective application of the proposed RMS calculation equation demands the determination of the crest factor [12]. It is defined as a modulus of the ratio of the maximum instantaneous peak value of the frequency-weighted acceleration signal to its RMS value. If the crest factor is higher than 9, the proposed basic evaluation method may underestimate the vibration level and therefore is considered invalid. Standard is equipped with additional evaluation - running RMS method, which considers occasional shocks and transient vibrations. Integration of the acceleration in a short time period t over the measurement period T is applied. Maximum transient vibration value (MTVV) expresses the peak acceleration magnitude and is often used to convert the overall vibration signal into one value to characterize the ride quality. However, since the riding vehicle accelerations are not steady-state, the resulting RMS value depends on the measurement duration.

For this reason, the vibration dose value (VDV) is used. This is a onefold and robust method, which is not affected by averaging. VDV represents an indication of the perceived doses and increases for a longer acquisition time. Therefore, the relative difference is more important than the actual value. VDV is generally reliable and robust for stationary and non-stationary accelerations. ISO 2631-1 [12] provides approximate values to indicate likely reactions to various magnitudes of overall vibration total values in public transport, presented in Table 2.

It is essential to separate absolute values of objective metrics achieved during simulations and vibration-induced discomfort experienced by vehicle occupants [27]. Difference thresholds (DT) can be used for this purpose. Here DT can be defined as "the minimum change in the magnitude of the whole-body vibration required for the seat occupant to perceive the change in magnitude" [28]. Commonly DT is marked as "Relative DT" and can be calculated in accordance with [27]:

$$\text{Relative DT} = \frac{\Delta I}{I} \cdot 100, \quad (4)$$

where I is the reference stimulus magnitude (intensity).

FIGURE 2 The weighting factor for vibrations in a vertical direction.

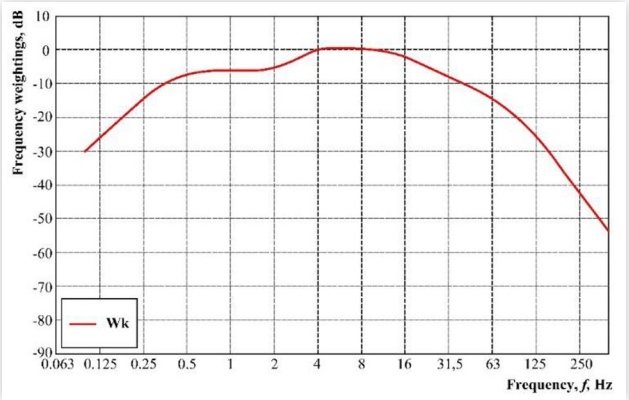

TABLE 2 Discomfort limits according to ISO 2631-1.

Discomfort Limit (m/s²)	Approx. Indications
< 0.315	not uncomfortable
0.315-0.63	a little uncomfortable
0.5-1.0	fairly uncomfortable
0.8-1.6	uncomfortable
1.25-2.5	very uncomfortable
> 2.0	extremely uncomfortable

3. Ride Comfort Evaluation

3.1. Sinusoidal Excitation

The input of the sinusoidal road profile for the left rear wheel was used during the whole vehicle simulation. The speeds of 15.3, 30.6, 61.2 and 122.4 km/h were maintained for each straight driving simulation generating the excitation frequency of 2.5, 5.0, 10 and 20 Hz, respectively, since the wavelength of the sinusoidal road profile was kept at 1.7 m for all cases. According to the studies, where authors analyze subjective human sensation to artificial vibration sources, these frequencies for wheel excitation were selected [27, 28]. The summarized results of sprung and unsprung mass vertical accelerations and exciting wheel normal force for vehicle default and IWM model cases are presented in Table 3.

As it was mentioned in the Introduction, IWM causes the increase of the unsprung mass that influences the whole vehicle dynamic. The first two row groups of Table 3 (for default and IWM model) corresponds to ride comfort level by unweighted and weighted sprung mass acceleration. RMS values increase intensively with higher-order for the IWM model always, moving from 2.5 Hz up to 10 Hz. The reverse order between default and IWM model was found at 20 Hz excitation, meaning that occupants will have slightly better comfort with the IWM at the sprung mass in such riding conditions. However, the acceleration RMS values (Table 3) show unsprung mass influence on sprung mass behavior as it usually works in broader frequency. The reduced natural frequency of the IWM model causes that, in this case, the model is less sensitive for the highest applied excitation frequencies. Therefore, the RMS values of sprung mass vertical acceleration are lower for the IWM case at 20 Hz as opposed to 2.5 Hz, 5.0 Hz and 10 Hz cases.

The rising tendency for all RMS values in Table 3 up to 10 Hz excitation is constant and consistent. This includes the proportion between default and IWM model cases. Despite the fact that the discomfort level at 20 Hz swapped and became higher for the default model, the vehicle road holding behavior is ambiguous. The vertical acceleration of the rear left unsprung mass (the one that was excited and got additional mass of IWM) at 20 Hz became higher for the default model; however, RMS values of the wheel normal force are still higher for IWM. The wheel normal force is one of the main variables affecting the tire-road grip; therefore, the vehicle handling is analyzed more detail in Section 4.

TABLE 3 The values of comfort simulation, sinusoidal excitation.

	2.5 Hz	5.0 Hz	10 Hz	20 Hz
	RMS of Sprung Mass Vertical Acceleration (Unweighted) (m/s^2)			
Default model	0.3979	0.5987	0.9665	0.4014
IWM model	0.4190	0.6644	1.101	0.2552
Absolute difference	0.021	0.066	0.135	0.146
	RMS of Sprung Mass Vertical Acceleration (W_k Weighted) (m/s^2)			
Default model	0.5768	0.5513	0.9349	0.5955
IWM model	0.6072	0.6121	1.0722	0.3797
Absolute difference	0.030	0.061	0.1373	0.216
	RMS of Unsprung Mass Vertical Acceleration (m/s^2)			
Default model	2.3354	11.0156	56.0778	73.1454
IWM model	2.4321	12.0869	66.1305	33.5504
	RMS of Wheel Normal Force (N)			
Default model	5663.0	5554.7	5980.5	6291.9
IWM model	6014.9	5939.4	7472.8	6402.6

3.2. Belgian Paving

During the next simulation, Belgian paving has been used for wheel stochastic excitation. It can be seen that for all cases, the unweighted RMS value is higher than 2. For driving velocities of 20 and 50 km/h, the RMS values are higher than 2; for 30 and 40 km/h, RMS are less than 2 (Table 4). According to [12] (Table 2), such a ride would be very uncomfortable.

In [27], the authors used the same vehicle and evaluated different thresholds for unweighted RMS. These values are 0.062 m/s^2 for a smooth road and 0.082 m/s^2 for a rough road. This difference feels 50% of test persons at a 79.4% probability level. It can be seen that a new vehicle corner design with an IWM caused barely noticeable vibration discomfort; the RMS increase is similar to DT values. In the case of sinusoidal excitation at 20 Hz, the RMS value even decreased. Moreover, vehicle handling can be negatively affected at this frequency due to an unstable tyre-road contact. The important assumption: in provided research RMS on vehicle CoG, is presented in experimental works, authors measure RMS on the seat, values cannot be compared directly.

TABLE 4 The values of comfort simulation, Belgian pavement.

	20 km/h	30 km/h	40 km/h	50 km/h
	RMS of Sprung Mass Vertical Acceleration (Unweighted) (m/s^2)			
Default model	2.765	2.103	2.046	2.401
IWM model	2.795	2.106	2.047	2.493
Absolute difference	0.030	0.003	0.001	0.092
	RMS of Sprung Mass Vertical Acceleration (W_k Weighted) (m/s^2)			
Default model	2.012	1.882	1.894	2.027
IWM model	2.085	1.905	1.952	2.118
Absolute difference	0.073	0.023	0.058	0.091

4. Vehicle Handling Evaluation

Three maneuvers were selected for vehicle handling evaluation in default and in-wheel model cases: i) open-loop type straight-line braking; ii) steady-state constant radius cornering; iii) closed-loop type double lane change.

4.1. Straight-Line Braking

Road pavement with an elevation of class D [29] and Belgian paving was selected to evaluate the influence of IWM on straight-line braking performance. The final value of 90% of maximal brake torque with 0.5 s step duration from initial speeds of 60 km/h and 90 km/h were used for vehicle hard braking simulation. The braking distance is the main parameter of braking performance; however, the Dynamic Load Coefficient (DLC) was also calculated for each braking case as it is the essential road holding parameter evaluating the tire grip on the rough road [30, 31]. The obtained results are presented in Table 5.

No changes for vehicle corner geometry were involved in these simulations as it is a straight-line maneuver. Hence, a straight and ground-perpendicular position is the best for the wheel-pavement contact.

As expected, the deterioration of braking performance for IWM architecture is more noticeable on the road with higher roughness levels. A longer braking distance and higher DLC values for both initial speeds prove the negative effect of the in-wheel architecture on rough roads; however, a smooth pavement does not significantly influence the braking performance compared to the default chassis construction.

4.2. Steady-State Cornering

Steady-state cornering [32] at 60 m radius with increasing vehicle speed from 10 km/h to 80 km/h on a smooth (class B) road pavement with 0.8 friction coefficient was performed on the second stage of vehicle handling evaluation. Presented vehicle corner architecture allows a dynamic wheel positioning with suspension-integrated actuators; therefore, camber angle (+/- 3 deg.) and toe angle (+/-1 deg.) change for rear axle wheels was involved in vehicle steady-state cornering simulations as it is a possible option for improving tire grip and vehicle lateral dynamics performance.

TABLE 5 Braking performance for different vehicle corner architectures.

	Class D		Belgian Paving	
	60 km/h	90 km/h	60 km/h	90 km/h
	Braking distance (m)			
Default model	16.33	43.11	17.44	44.60
IWM model	16.50	42.31	17.89	45.41
Difference	+0.17	-0.80	+0.45	+0.81
	DLC			
Default model	0.641	0.723	0.814	0.835
IWM model	0.659	0.721	0.880	0.904
Difference	+0.018	-0.002	+0.066	+0.069

FIGURE 3 Vehicle body side-slip angle during double lane change maneuver for IWM model architecture.

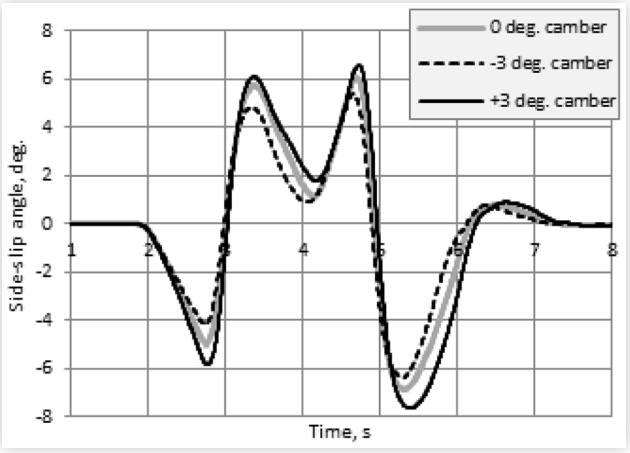

The vehicle body side-slip angle had a lower increasing tendency with negative wheel camber at increasing vehicle speed during cornering. A slightly lower drop of yaw rate when reaching a critical cornering stage was also found for negative camber. The wheel toe control did not show a significant positive effect during the cornering maneuver. Therefore, the negative camber made a slightly more positive impact on the handling by the IWM corner architecture as compared to the default model case.

4.3. Double Lane Change

The closed-loop type double lane change maneuver [33] was selected to evaluate the third stage of vehicle handling. This maneuver imitates real-life situations and is usual for secondary vehicle dynamics simulation [34]. The same road as in the previous cornering maneuver (class B and 0.8 friction coefficient) was used in this evaluation for default and IWM cases.

As in the last maneuver, negative camber has shown slight improvement for vehicle handling. It is recognized in smaller steering wheel magnitudes, lower yaw rate and body side-slip angle, which decreases by 0.8, 0.87, 0.99, 0.17 degrees depending on the stage of lane change (Fig. 3). The same positive effect for handling is recognized for both default and IWM model cases.

Toe angle correction did not significantly benefit default or IWM model cases as only slight body side-slip angle reduction was recognized with a positive toe.

5. Conclusions

An electric vehicle architecture with wheel corners equipped with in-wheel motors (IWM) was analyzed in this paper, taking into account objective occupant comfort evaluation. A multi-body model of a sport utility vehicle with a new corner design including IWM and active wheel camber/toe angle

control was developed for ride and handling simulations. From the perspective of vertical vehicle dynamics, larger wheel mass with a motor mounted causes a lower natural frequency of unsprung mass only; however, whole vehicle ride simulations showed ambiguous results for objective comfort evaluation. RMS value of the weighted vertical acceleration of sprung mass increased with increasing pavement excitation from 2.5 to 10 Hz with higher IWM architecture values than the default one. At 20 Hz frequency, excitation is relatively far for both sprung and unsprung mass natural frequencies that cause lower acceleration response; however, IWM architecture demonstrated lower discomfort values at this excitation. Comfort level on Belgian paving showed slightly higher sprung vertical mass acceleration for IWM case at 20-50 km/h speed performed simulations.

As a high variation of normal wheel force was recognized at sinusoidal wheel excitation cases, vehicle handling evaluation using straight-line braking, steady-state cornering and double lane change simulation maneuvers were performed. The deterioration of braking performance with IWM architecture was noticeable in the rough road (Belgian paving) simulation, while the smoother road has not caused a longer braking distance than the default model.

The option of active wheel camber/toe angle control from presented vehicle corner architecture was also utilized to evaluate transversal vehicle dynamics. Smooth enough pavement (B class) was used to avoid different vertical excitation aspects. In such conditions, vehicle corner architecture with in-wheel motor does not cause significant deterioration; moreover, 3 deg. negative camber showed a positive impact on vehicle handling, and an active asymmetrical wheel geometry regulation, including toe angle, is a promising direction for future research.

References

1. Borroni-Bird, C., "Making the Case for In-Wheel Motors," SAE International, *Automotive Engineering*, July/August, 15-19, 2021 (accessed on October 5, 2021).
2. Akaho, D., Nakatsu, M., Katsuyama, E., Takakuwa, K. et al., "Development of Vehicle Dynamics Control System for In-Wheel-Motor Vehicle," in *Proc. JSAE Annual Congress (Spring)*, Yokohama, Japan, May 2010, 20105533, 1-6.
3. Murata, S., "Innovation by In-Wheel-Motor Drive Unit," *Vehicle System Dynamics: Int. J. Vehicle Mechanics and Mobility* 50, no. 6 (2012): 807-830, doi:10.1080/00423114.2012.666354.
4. Young, D.A., Shabana, M.D., Borroni-Bird, C.E., Chernoff, A.B. et al., Vehicle wheel system, GM Global Technology Operations LLC. U.S. Patent 7,398,846, July 15, 2008.
5. Zetterström, S., "Electromechanical Steering, Suspension, Drive and Brake Modules," in *Proceedings of the 56th IEEE Vehicular Technology Conference,* Vancouver, Canada, 3:1856-1863, September 2002, doi:10.1109/VETECF.2002.1040538.
6. Murata, S., "Vehicle Dynamics Innovation with In-Wheel Motor," SAE Technical Paper 2011-39-7204 (2011), doi:10.4271/2011-39-7204.
7. Hu, J.-S., Lin, X.-C., Yin, D., and Hu, F.-R., "Dynamic Motion Stabilization for Front-Wheel Drive In-Wheel Motor Electric Vehicles," *Advances in Mechanical Engineering* 7, no. 12 (2015): 1-11, doi:10.1177/1687814015623694.
8. Jiang, X., Chen, L., Xu, X., Cai, Y. et al., "Analysis and Optimization of Energy Efficiency for an Electric Vehicle with Four Independent Drive In-Wheel Motors," *Advances in Mechanical Engineering* 10, no. 3 (2018): 1-9, doi:10.1177/1687814018765549.
9. Anderson, M. and Harty, D., "Unsprung Mass with In-wheel Motors - Myths and Realities," in *Proceedings of the 10th International Symposium on Advanced Vehicle Control*, Loughborough, UK, 2010.
10. Hurdwell, R. and Anderson, M., "Dynamics of Vehicles with In-wheel Motors," in *Proc. of Vehicle Dynamics and Control Seminar*, Cambridge, UK, 2011.
11. Nie, S., Zhuang, Y., Chen, F., Wang, Y. et al., "A Method to Eliminate Unsprung Adverse Effect of In-Wheel Motor-Driven Vehicles," *Journal of Low Frequency Noise, Vibration and Active Control* 37, no. 4 (2018): 955-976, doi:10.1177/1461348418767096.
12. "Shock - Evaluation of Human Exposure to Whole-Body Vibration - Part 1: General Requirements," International Organization for Standardization, ISO 2631-1: 1997, Rev 2, 31. Available online: https://www.iso.org/standard/7612.html (accessed on July 28, 2021).
13. Yang, Z., Yong, C., Li, Z., and Kangsheng, Y., "Simulation Analysis and Optimization of Ride Quality of In-Wheel Motor Electric Vehicle," *Advances in Mechanical Engineering* 10, no. 5 (2018): 1-10, doi:10.1177/1687814018776543.
14. Salami, H., Abbasi, M., Zand, T.F., Fard, M. et al., "Anew Criterion for Comfort Assessment of In-Wheel Motor Electric Vehicles," *Journal of Vibration and Control* 0, no. 0 (2020): 1-13, doi:10.1177/1077546320977187.
15. Nagaya, G., Wakao, Y., and Abe, A., "Development of an In-Wheel Drive with Advanced Dynamic-Damper Mechanism," *JSAE Rev* 24, no. 4 (2003): 477-481. https://doi.org/10.1016/S0389-4304(03)00077-8.
16. Meng, L., Zou, Y., Qin, Y., and Hou, Z., "A New Electric Wheel and Optimization on Its Suspension Parameters," *Proc IMechE Part D: J Automobile Engineering* 234, no. 12 (2020): 2759-2770, doi:10.1177/0954407020921736.
17. Shi, P., Shi, P., Yan, C., Zhang, R. et al., "Analysis of the Electric Wheel Vibration Reduction System of a Wheel-Hub Motor-Driven Vehicle," *Proc IMechE Part C: J Mechanical Engineering Science* 233, no. 3 (2019): 848-856, doi:10.1177/0954406218766373.
18. Kulkarni, A., Ranjha, S.A., and Kapoor, A., "A Quarter-Car Suspension Model for Dynamic Evaluations of an In-Wheel Electric Vehicle," *Proc IMechE Part D: J Automobile Engineering* 232, no. 9 (2018): 1139-1148, doi:10.1177/0954407017727165.
19. Wang, Y., Li, Y., Sun, W., and Zheng, L., "Effect of the Unbalanced Vertical Force of a Switched Reluctance Motor on the Stability and the Comfort of an In-Wheel Motor Electric Vehicle," *Proc IMechE Part D: J Automobile Engineering* 229, no. 12 (2015): 1569-1584, doi:10.1177/0954407014566438.

20. "Guide to Measurement and Evaluation of Human Exposure to Whole-Body Mechanical Vibration and Repeated Shock," British Standards Institution, BS 6841:1987, ISBN0580160491. Available online: https://shop.bsigroup.com/products/guide-to-measurement-and-evaluation-of-human-exposure-to-whole-body-mechanical-vibration-and-repeated-shock?pid=000000000000171912 (accessed on July 28, 2021).
21. Griffin, M.J., "Discomfort from Feeling Vehicle Vibration," *Vehicle System Dynamics* 45, no. 7-8 (2007): 679-698. https://doi.org/10.1080/00423110701422426.
22. Kumar, K., Pal, S., and Sethi, R., "Objective Evaluation of Ride Quality of Road Vehicles," SAE Technical Paper 990055 (1999). https://doi.org/10.4271/990055.
23. Little, E., Handrickx, P., Grote, P., Mergay, M. et al., "Ride Comfort Analysis: Practice and Procedures," SAE Technical Paper 990053 (1999). https://doi.org/10.4271/990053.
24. Previati, G., Gobbi, M., and Mastinu, G., "Subjective-Objective Ride Comfort Assessment of Farm Tractors," SAE Technical Paper 2016-01-1437 (2016). https://doi.org/10.4271/2016-01-1437.
25. Janeway, R., "Human Vibration Tolerance Criteria and Applications to Ride Evaluation," SAE Technical Paper 750166 (1975). https://doi.org/10.4271/750166.
26. Franceschini, F., Vilela, D., and Volney, M., "Automotive Suspension Calibration," SAE Technical Paper 2002-01-3393 (2002). https://doi.org/10.4271/2002-01-3393.
27. Gräbe, R.P., Kat, C.-J., van Staden, P.J., and Els, P.S., "Difference Thresholds for a Vehicle on a 4-Poster Test Rig," *Applied Ergonomics*, 87(4):1-11, 2020, https://doi.org/10.1016/j.apergo.2020.103115.
28. Forta, N.G., Morioka, M., and Griffin, M.J., "Difference Thresholds for the Perception of Whole-Body Vertical Vibration: Dependence on the Frequency and Magnitude of Vibration," *Ergonomics* 52, no. 10 (2009): 1305-1310, doi:10.1080/00140130903023709.
29. "Mechanical Vibration - Road Surface Profiles - Reporting of Measured Data," International Organization for Standardization, ISO 8608:2016, Rev 2, 36. Available online: https://www.iso.org/standard/71202.html (accessed on September 25, 2021).
30. Cebon, D., *Handbook of Vehicle-Road Interaction* (CRC Press, 1999), ISBN:9789026515545
31. Žuraulis, V., Sivilevičius, H., Šabanovič, E., Ivanov, V. et al., "Variability of Gravel Pavement Roughness: An Analysis of the Impact on Vehicle Dynamic Response and Driving Comfort," *Appl. Sci.* 11(16):1-18, 2021, 7582, https://doi.org/10.3390/app11167582.
32. "Passenger Cars - Steady-State Circular Driving Behaviour - Open-Loop Test Methods," International Organization for Standardization, ISO 4138:2021, Rev 5, 32. Available online: https://www.iso.org/standard/81710.html (accessed on October 15, 2021).
33. "Passenger Cars — Test Track for a Severe Lane-Change Manoeuvre — Part 1: Double Lane-Change," International Organization for Standardization, ISO 3888-1:2018, Rev 2, 6. Available online: https://www.iso.org/standard/67973.html (accessed on August 15, 2021).
34. Kutluay, E. and Winner, H., "Validation of Vehicle Dynamics Simulation Models - A Review," *Vehicle System Dynamics* 52, no. 2 (2014): 186-200, doi:10.1080/00423114.2013.868500.

Contact Information

Viktor Skrickij,
Transport and Logistics Competence Centre
Saulėtekio al. 11, office SRC-309, LT-10223 Vilnius, Lithuania.
+370 5 2744981
viktor.skrickij@vilniustech.lt
www.vilniustech.lt

Acknowledgments

This research was funded from the European Union Horizon 2020 Framework Program, Marie Skłodowska-Curie actions, under grant agreement no. 872907.

Definitions/Abbreviations

IWM - In-wheel motor
RMS - Root-mean-square
CoG - Center of Gravity
OEM - Original equipment manufacturer
CAD - Computer-Aided Design
3D - Three-dimensional
SUV - Sport Utility Vehicle
MTVV - Maximum transient vibration value
VDV - Vibration dose value
DT - Difference thresholds
DLC - Dynamic Load Coefficient

ISSN 0148-7191